Live-cell imaging shows apoptosis initiates locally and propagates as a wave throughout syncytiotrophoblasts in primary cultures of human placental villous trophoblasts

Mark S. Longtine[a,*], **Aaron Barton**[a,b], **Baosheng Chen**[a], and **D. Michael Nelson**[a]

[a]Department of Obstetrics and Gynecology, Washington University School of Medicine St. Louis, MO, 63110, USA

Abstract

Human placental villi are surfaced by the syncytiotrophoblast, a multinucleated, epithelial-cell layer that functions in maternal-fetal exchange. Mononucleated cytotrophoblasts are subjacent to the syncytiotrophoblast. Using confocal fluorescence microscopy of third-trimester villi, we previously found that cytotrophoblasts are often interdigitated into the syncytiotrophoblast, that cytotrophoblasts undergo caspase-mediated apoptosis, and that apoptosis is much lower, and perhaps completely inhibited, in intact syncytiotrophoblast lacking fibrin-type fibrinoid. Previous analysis of primary cultures of human trophoblasts also indicated lower levels of apoptosis in syncytiotrophoblast compared to cytotrophoblasts. Here, using confocal microscopy we find that cultured cytotrophoblasts and syncytiotrophoblasts display complex structural relationships, as *in vivo*, and that apoptosis of a cytotrophoblast or syncytiotrophoblast does not induce apoptosis of adjacent trophoblasts. Using live-cell imaging of mitochondrial depolarization and nuclear condensation in cultured syncytiotrophoblasts, we show apoptosis initiates in a localized region and propagates radially at ~five μm/min with no loss of velocity until the entire syncytium has undergone apoptosis. The rate of propagation is similar in cases of spontaneous apoptosis and in apoptosis that occurs in the presence of cobalt chloride or rotenone, two inducers of apoptosis. We suggest that inhibition of syncytiotrophoblast apoptosis *in vivo* is important to prevent widespread syncytiotrophoblast death, which would result in placental dysfunction and contribute to poor pregnancy outcomes.

Keywords

placenta; apoptosis; syncytiotrophoblast; cytotrophoblast

1. Introduction

The placenta is a transient organ that is essential for growth and development of the human fetus. This organ elaborates villous trees that are bathed in maternal blood, mediate maternal-fetal exchange, and secrete hormones pivotal to pregnancy. A multinucleated

*Corresponding Author: Department of Obstetrics and Gynecology, Washington University School of Medicine, Campus Box 8064, 4566 Scott Ave., St. Louis, MO, 63110, Tel: (314) 362-3150, Fax: (314) 362-8580, longtine@wudosis.wustl.edu.
[b]Current address: AUC School of Medicine, Sint Maarten, Netherland Antilles

syncytium, the syncytiotrophoblast, comprises the outer epithelial layer of villi and thus is the primary site of interaction between the mother and fetus. Current evidence suggests the human syncytiotrophoblast consists of a single, continuous cytoplasm [1], at term containing $\sim 5 \times 10^{10}$ nuclei, a volume of ~ 50 cm^3 and a surface area of ~ 11 m^2 [2,3]. Subjacent to the syncytiotrophoblast are mononucleated cytotrophoblasts, the second villous trophoblast phenotype. Cytotrophoblasts are able to undergo cell division and fuse with the syncytium, thereby allowing syncytiotrophoblast growth and repair.

Preeclampsia, intrauterine growth restriction (IUGR), or preeclampsia with IUGR, occur in about 10% of pregnancies [4,5]. Oxidative and nitrative stress and elevated levels of TNF-α are characteristic of such complicated pregnancies, and these stressors are believed to contribute to placental dysfunction [6–8]. To address the hypothesis that elevated trophoblast apoptosis may contribute to these pathologies of pregnancy, we recently used Z-stack confocal microscopy and staining for trophoblast plasma membranes with E-cadherin and for markers of apoptosis to investigate apoptosis in both phenotypes of villous trophoblasts from third-trimester pregnancies [9,10]. We found that cytotrophoblasts and the syncytiotrophoblast showed complex structural relationships in villi, with one-third of the cytotrophoblasts deeply interdigitated into the syncytiotrophoblast. In term, normotensive pregnancies, about one percent of cytotrophoblasts were positive for markers of apoptosis. In pregnancies complicated by preeclampsia, IUGR or both, cytotrophoblast apoptosis was significantly elevated (to 4–8%), suggesting apoptosis in this stem-cell like population may contribute to placental dysfunction in these pregnancies.

Remarkably, we did not detect any evidence in villi for caspase-mediated apoptosis in intact regions of syncytiotrophoblast devoid of fibrin-containing fibrinoid, even in complicated pregnancies [9,10]. During *in vitro* culture, primary human cytotrophoblasts undergo spontaneous differentiation and fusion, with ~80% of the nuclei in syncytia after 52 h of culture in 20% O$_2$ [11–13]. Compared to cultured cytotrophoblasts, cultured syncytiotrophoblasts express lower caspase protein levels [14], down-regulate p53 in conditions of low oxygen [11], and are more resistant to apoptosis [11,14–16]. Together, these results suggest apoptosis is repressed in syncytiotrophoblasts, perhaps to prevent widespread death of the syncytium.

Here, we use fixed-cell imaging of cultured primary human trophoblasts to investigate the structural relationships of cytotrophoblasts and syncytiotrophoblasts *in vitro*. We also use fixed-cell and live-cell imaging of cultured primary human trophoblasts to test the hypothesis that apoptosis, once initiated within a syncytium, progresses throughout the entire syncytium without constraint.

2. Materials and methods

2.1. Isolation, culture and immunofluorescence of primary human trophoblasts

Primary human trophoblasts (PHTs) were isolated from placentas obtained after C-section delivery of term, uncomplicated, singleton pregnancies, as described [11]. PHTs were plated at 350,000 cells/cm^2 on tissue-culture-treated plastic plates and cultured in DMEM containing 10% fetal bovine serum, 20 mM HEPES pH 7.4, and penicillin/streptomycin in a 5% CO$_2$/air atmosphere, as described previously [11], with daily media changes. Cells were allowed to attach for 4 h, washed to remove unattached cells and syncytial fragments, and this time was designated as hour zero. Cells were fixed at 76 h with 4% w/v paraformaldehyde for 30 min, permeabilized and stained for DNA, E-cadherin (Abcam, Cambridge, MA), cleaved cytokeratin 18 (clCyt18; Roche, Indianapolis, IN), or cleaved PARP (clPARP; Cell Signaling Technology, Danvers, MA) and examined by confocal

microscopy using image optimization and 10 or more optical Z-stacks of < 0.5-μm spacing, as described previously [9].

2.2. Live-cell imaging

PHTs were cultured as described above. As noted in the text and Figure legends, after 76 h culture, cells were either labeled for 1 h at 37°C in medium with 25 μM JC-1 (Sigma), washed, and imaged in fresh medium with 0.5 μM JC-1 or with JC-1 in the presence of either 100 μM cobalt chloride (CoCl$_2$; Sigma) or 2 μM rotenone (Sigma), washed, and imaged in medium with 0.5 μM JC-1 and, if used, the same CoCl$_2$ or rotenone concentrations. JC-1 is a fluorescent dye that accumulates in mitochondria. In polarized mitochondria, JC-1 aggregates and is strongly fluorescesent at ~590 nm. Upon mitochondrial depolarization, JC-1 disaggregates, resulting in a reduced fluorescence at ~590 nm. Plates were placed on the stage of a Nikon T2000 inverted microscope, which used an X-, Y-, Z-position programmable motorized stage (ASI, Eugene, OR) and Sutter shutters (Novato, CA) to allow rapid switching between phase contrast and fluorescence microscopy, which used a rhodamine filter set (Chroma Technology, Bellows Falls, VT), with the system managed using Metamorph software (Molecular Devices, Sunnyvale, CA). The microscope and samples were housed within a plexiglass incubation box and temperature maintained at 37°C using a heated air system (both from Life Imaging Services, Basel, Switzerland) with a continuous flow of 5% CO$_2$/air over the sample maintained within a small glass chamber that covered the plate. After 30 min on the microscope stage to allow temperature equilibration, images of 1600×1200 pixels (547 μm $\times$ 448 μm) were acquired every 5 min for > 10 h using a 10X lens and a Retiga RTV2000 camera (QImaging, Surray, BC Canada). Only linear functions of ImageJ (NIH) were used to adjust images. Images were adjusted for photobleaching that occurred during the 10 h of imaging, which was typically   40% of signal intensity, and the signal intensity of regions of interest measured using the Multimeasure plugin of ImageJ.

2.3. Statistical analyses

Comparisons of the rates of progression of apoptosis between culture conditions was done using Anova with Tukey's *post hoc* test, with $p < 0.05$ as significant.

3. Results

3.1. Fixed-cell imaging of trophoblasts and trophoblast apoptosis

To examine apoptosis in cultured trophoblasts in fixed cells, we used confocal imaging to distinguish cytotrophoblasts from the syncytiotrophoblasts after staining for E-cadherin, which marks plasma membranes, and DNA (Fig. 1; see serial confocal sections in Supplementary movie 1). Cytotrophoblasts on the periphery of a syncytium were visible (Fig. 1, green arrow) as were cytotrophoblasts that partially or completely overlaid (Fig. 1, red arrow) or underlaid the syncytium (not shown), or even that were surrounded by syncytium (Fig. 1, white arrow). To identify apoptotic cells, we stained for E-cadherin, DNA, and for cleaved cytokeratin 18 (clCyt18) and cleaved poly (ADP-ribose) polymerase (clPARP), two markers for caspase-mediated apoptosis. Confocal microscopy showed that a subset of cytotrophoblasts expressed clCyt18 (Fig. 2A, B, red arrows; see Supplementary movie 2), with some of these apoptotic cytotrophoblasts adjacent to, overlaying, or underlaying, a syncytium (Fig. 2A, B). Cytotrophoblasts that were apoptotic but surrounded by regions of non-apoptotic syncytium were also identified (Fig. 2A, boxed region). Confocal Z-stack imaging was required to identify cytotrophoblasts expressing a marker of apoptosis, as the E-cadherin staining in these cells was less intense than in non-apoptotic cytotrophoblasts and typically was largely cytoplasmic rather than localized to the plasma membrane. This is similar to what we found in apoptotic cytotrophoblasts in term villi [9,10]

and likely reflects caspase-mediated cleavage of E-cadherin, resulting in E-cadherin becoming cytoplasmic [17,18]. DNA fragmentation and degradation were present in some apoptotic cytotrophoblasts, again consistent with descriptions of placental tissues [9,10].

Apoptotic syncytiotrophoblast regions were also apparent, as indicated by multinucleated regions lacking interstitial E-cadherin and containing high levels of clCyt18 or clPARP (Fig. 2C, D; see Supplementary movie 3). In all cases of apoptotic syncytium identified in fixed cells, the marker for apoptosis was present throughout the entire syncytium and was not restricted to subregions of an individual syncytium. Regions of apoptotic syncytiotrophoblasts in the cultures typically displayed condensed nuclei with unevenly distributed DNA (Fig. 2C), consistent with pyknosis [19].

Notably, syncytiotrophoblasts and cytotrophoblasts undergoing apoptosis did not influence the presence or absence of apoptosis in adjacent cells: apoptotic cytotrophoblasts were in contact with non-apoptotic syncytia (Fig. 2 A, B) and apoptotic syncytia were in contact with non-apoptotic cytotrophoblasts (Fig. 2C, D).

3.2. Live-cell imaging of syncytiotrophoblast apoptosis

The above results using fixed cells showed that apoptosis occurred throughout a syncytium, suggesting two possibilities for the progression of apoptosis in syncytiotrophoblasts *in vitro*. First, apoptosis may occur simultaneously throughout the syncytium, or, second, apoptosis may initiate in one or more localized regions and then propagate throughout the syncytium. To investigate these possibilities, we used JC-1, a potential-dependent fluorescent dye that accumulates in polarized mitochondria and whose fluorescence is decreased by mitochondrial depolarization that occurs during apoptosis. After 76 h of culture, JC-1-labeled trophoblasts were imaged by fluorescence and phase-contrast microscopy to follow mitochondrial polarization and condensation of nuclear DNA, respectively, which are two hallmarks of apoptosis [19]. Spontaneous events of apoptosis in syncytiotrophoblast were captured, as reflected by loss of JC-1 signal and nuclear condensation (Fig. 3A). In all cases, apoptosis initiated in a localized region (Fig. 3, i, t = 55 min), with mitochondrial depolarization and nuclear condensation occurring in tandem within the 5 min time resolution of the imaging. The two markers of apoptosis propagated outwards as a wave (Fig. 3, See Supplementary Movie 4), moving at ~4.5 μm/min (4.40 ± 1.74, n = 8 events), ultimately spreading throughout the entire syncytium, without spreading to adjacent trophoblasts. There was a small, transient elevation in the JC-1 signal just in front of the wave of mitochondrial depolarization (Fig. 3B, arrows). Although nuclei underwent condensation, apoptotic syncytiotrophoblasts otherwise appeared remarkably stable: > 5 h post nuclear condensation, we did not detect fragmentation or degradation of nuclei or blebbing of the plasma membrane, which is seen in other cell types [20,21].

There were also dispersed, defined areas where the JC-1 signal persisted, and usually increased ~ 2-fold, subsequent to the loss of the JC-1 signal during syncytiotrophoblast apoptosis (Fig. 3, cyto). We propose these regions are due to overlaying, underlaying, or captured cytotrophoblasts (see *Discussion*).

We next asked if apoptosis that occurs in the presence of inducers initiates in a single region and progresses throughout the syncytium, as we noted for spontaneous events. Thus, we carried out live-cell imaging of syncytiotrophoblasts exposed to cobalt chloride (CoCl$_2$) and rotenone, two inducers of apoptosis. CoCl$_2$ is a hypoxia mimetic that increases apoptosis of cultured trophoblasts [11] and other cells by altering transcription of HIF1α and by increasing reactive oxygen species (ROS) [22,23]. Rotenone inhibits electron transport through complex 1 [24,25], resulting in increased ROS and increased apoptosis [26–28]. In the presence of CoCl$_2$, apoptosis always initiated in a localized region of a syncytium and

propagated outwards at 4.71 ± 1.77 µm/min (n = 5 events), which did not differ significantly ($p = 0.75$) from the rate of propagation of spontaneous apoptosis. Similarly, in the presence of rotenone, apoptosis initiated in a localized region of a syncytium and propagated outwards at 3.73 ± 0.90 µm/min (n = 5 events), which again did not differ significantly ($p = 0.7$) from the rate of propagation of spontaneous apoptosis.

4. Discussion

Our data are consistent with a model that apoptosis, once initiated within a syncytium, progresses throughout the entire syncytium without constraint. Although cultured primary human cytotrophoblasts and syncytiotrophoblasts show complex structural relationships with each other, similar to what is observed in the trophoblast bilayer of term human placental villi, apoptosis in syncytiotrophoblasts or cytotrophoblasts does not induce apoptosis in adjacent trophoblasts. Fixed-cell imaging indicates that apoptosis, measured by caspase-cleaved proteins in the cytoplasm or nucleus, always occurs throughout the syncytiotrophoblast. Live-cell imaging indicates that apoptosis initiates within a localized region of a syncytium and propagates as a wave of mitochondrial depolarization and nuclear condensation. This wave propagates at a similar rate whether occurring spontaneously or in the presence of exogenous stimuli, appears self-reinforcing, and leads to apoptosis throughout the syncytium. We speculate that the potential for unconstrained spreading is why apoptosis is highly repressed in syncytiotrophoblasts *in vivo*.

We found no evidence of transmission of apoptotic signals between trophoblasts despite the known role of gap-junctions in trophoblast fusion [29–31] and findings in other systems of the bystander effect, which is when death of a cell, or a portion of a tissue, induces death of nearby cells (reviewed in [32]) via gap junction-independent or -dependent mechanisms [33–35]. Similarly, there is an apparent absence of spreading of apoptosis from apoptotic cytotrophoblasts to adjacent syncytiotrophoblast in term [9,10] and first-trimester villi [36], which may be important in limiting trophoblast apoptosis *in vivo*.

We noted a transient increase in JC-1 fluorescence in the syncytiotrophoblast just in front of the apoptotic wave. We also noted a persistent increase in discrete areas subsequent to loss of JC-1 fluorescence of a syncytium. These discrete areas of increased JC-1 fluorescence are likely due to cytotrophoblasts that overlaid, underlaid, or were surrounded by syncytiotrophoblast: the frequency and shape of these regions were consistent with those of cytotrophoblasts detected by immunofluorescence of fixed cells and, in some cases (*e.g.*, Fig. 3, cyto), the cytotrophoblast cell border was detectable by phase contrast microscopy. A simple explanation for these findings is that JC-1 is released from the depolarizing mitochondria of the syncytium resulting in an increase in JC-1 concentration in the cytoplasm in front of the wave, resulting in a transient increase in JC-1 signal ahead of the moving wave, and that the syncytiotrophoblast undergoing apoptosis also releases JC-1 into the medium, allowing an increase of JC-1 levels in the mitochondria of nearby, non-apoptotic cytotrophoblasts.

Using fixed-cell microscopy and staining for caspase-cleaved cytokeratin 18 and PARP, we always detected apoptosis throughout an entire syncytium of cultured trophoblasts. Live-cell imaging of mitochondrial depolarization and nuclear condensation in syncytiotrophoblasts confirmed that apoptosis is unconstrained: apoptosis initiates in a localized region and spreads as a spatially coordinated wave at a rate of 4–5 µm/second without dissipation of velocity. This pattern of syncytiotrophoblast apoptosis occurred in standard condition (spontaneous events) and under inducing conditions (*i.e.*, in the presence of $CoCl_2$ or rotenone). Notably, the rate of propagation in cultured syncytiotrophoblasts is similar to what has been observed previously in mononucleated cells and syncytia generated by

artificial fusion of HeLa cells [37–39], including those initiated by activation of the intrinsic or extrinsic pathways of apoptosis [37,40,41].

Our data do not currently address the mechanism by which the original intracellular asymmetry arises that initiates the mitochondrial depolarization and apoptotic wave. Based on other systems, one possibility is that there is a localized increase of ROS generation by a mitochondrion or a few adjacent mitochondria. This locally elevated ROS production could then induce ROS release from nearby mitochondria by a phenomenon termed ROS-induced ROS release [37,40,42,43]. Because of its self-reinforcing nature, the wave of ROS, and thus mitochondrial depolarization, cytochrome c release [37,40], and apoptosis could be propagated from a small initial region throughout the syncytium.

In recent work [8,9], we used confocal microscopy to investigate apoptosis of third-trimester villous trophoblasts from placentas of women with normotensive pregnancies or pregnancies complicated with preeclampsia, IUGR, or both [8,9]. E-cadherin staining revealed non-apoptotic and apoptotic cytotrophoblasts could often be deeply interdigitated into the syncytiotrophoblast layer. Thus, in the absence of costaining for a membrane marker an apoptotic cytotrophoblast could be misidentified as indicating a localized region of apoptosis in the syncytiotrophoblast. Such misidentification may have occurred in some previous studies from our lab and other labs (for detailed discussion, see references [8,9]). Here, using E-cadherin staining of *in vitro* cultured trophoblasts, we find similar complex relationships of cytotrophoblasts and syncytiotrophoblasts: cytotrophoblasts can over- or underlay, or even be surrounded by, syncytia. Thus, in the absence of staining for a membrane marker, such apoptotic cytotrophoblasts could easily be misidentified as indicating a localized region of apoptosis in a syncytium.

The results described in this study, together with previous data [9–11,14,16], are consistent with the following hypothesis for placental villous trophoblast apoptosis. Cytotrophoblasts that are damaged by stressors respond by undergoing apoptosis, preventing the introduction of damaged cell components into the syncytiotrophoblast. The apoptotic cytotrophoblasts could be replaced by above-baseline division of the stem-cell-like population of cytotrophoblasts. In contrast, in syncytiotrophoblasts apoptosis is strongly inhibited, even under conditions of stress. Indeed, we suggest that the initiation of apoptosis is completely inhibited *in vivo* in syncytiotrophoblast with a continuous cytoplasm. Otherwise, once initiated, apoptosis would spread unconstrained, leading to death of the entire syncytiotrophoblast, placental dysfunction, and negative consequences for the fetus.

Supplementary Material

Refer to Web version on PubMed Central for supplementary material.

Acknowledgments

Abbreviations

clCyt18	cleaved cytokeratin 18
clPARP	cleaved poly-ADP-ribose polymerase

CoCl₂	

CoCl$_2$ cobalt chloride

O$_2$ oxygen

ROS   reactive oxygen species

References

1. Benirschke, K.; Kaufmann, P.; Baergen, R. Pathology of the human placenta (book). 5. 2006.

2. Mayhew TM, Leach L, McGee R, Ismail WW, Myklebust R, Lammiman MJ. Proliferation, differentiation and apoptosis in villous trophoblast at 13–41 weeks of gestation (including observations on annulate lamellae and nuclear pore complexes). Placenta. 1999; 20:407–22. [PubMed: 10419806]

3. Mayhew TM, Manwani R, Ohadike C, Wijesekara J, Baker PN. The placenta in pre-eclampsia and intrauterine growth restriction: studies on exchange surface areas, diffusion distances and villous membrane diffusive conductances. Placenta. 2007; 28:233–8. [PubMed: 16635527]

4. Rampersad R, Nelson DM. Trophoblast biology, responses to hypoxia and placental dysfunction in preeclampsia. Front Biosci. 2007; 12:2447–56. [PubMed: 17127254]

5. Scifres CM, Nelson DM. Intrauterine growth restriction, human placental development and trophoblast cell death. J Physiol. 2009; 587:3453–8. [PubMed: 19451203]

6. Burton GJ, Jauniaux E. Placental oxidative stress: from miscarriage to preeclampsia. J Soc Gynecol Investig. 2004; 11:342–52.

7. Haider S, Knofler M. Human tumour necrosis factor: physiological and pathological roles in placenta and endometrium. Placenta. 2009; 30:111–23. [PubMed: 19027157]

8. Redman CW, Sargent IL. Placental stress and pre-eclampsia: a revised view. Placenta. 2009; 30 (Suppl A):S38–42. [PubMed: 19138798]

9. Longtine MS, Chen B, Odibo AO, Zhong Y, Nelson DM. Caspase-mediated apoptosis of trophoblasts in term human placental villi is restricted to cytotrophoblasts and absent from the multinucleated syncytiotrophoblast. Reproduction. 2012; 143:107–21. [PubMed: 22046053]

10. Longtine MS, Chen B, Odibo AO, Zhong Y, Nelson DM. Villous trophoblast apoptosis is elevated and restricted to cytotrophoblasts in pregnancies complicated by preeclampsia, IUGR, or preeclampsia with IUGR. Placenta. 2012; 33:352–9. [PubMed: 22341340]

11. Chen B, Longtine MS, Sadovsky Y, Nelson DM. Hypoxia downregulates p53 but induces apoptosis and enhances expression of BAD in cultures of human syncytiotrophoblasts. Am J Physiol Cell Physiol. 2010; 299:C968–76. [PubMed: 20810912]

12. Humphrey RG, Smith SD, Pang L, Sadovsky Y, Nelson DM. Fibrin enhances differentiation, but not apoptosis, and limits hypoxic injury of cultured term human trophoblasts. Placenta. 2005; 26:491–7. [PubMed: 15950063]

13. Robins JC, Heizer A, Hardiman A, Hubert M, Handwerger S. Oxygen tension directs the differentiation pathway of human cytotrophoblast cells. Placenta. 2007; 28:1141–6. [PubMed: 17706280]

14. Yusuf K, Smith SD, Sadovsky Y, Nelson DM. Trophoblast differentiation modulates the activity of caspases in primary cultures of term human trophoblasts. Pediatr Res. 2002; 52:411–5. [PubMed: 12193677]

15. Crocker IP, Cooper S, Ong SC, Baker PN. Differences in apoptotic susceptibility of cytotrophoblasts and syncytiotrophoblasts in normal pregnancy to those complicated with preeclampsia and intrauterine growth restriction. Am J Pathol. 2003; 162:637–43. [PubMed: 12547721]

16. Hu C, Smith SD, Pang L, Sadovsky Y, Nelson DM. Enhanced basal apoptosis in cultured term human cytotrophoblasts is associated with a higher expression and physical interaction of p53 and Bak. Placenta. 2006; 27:978–83. [PubMed: 16376985]

17. Steinhusen U, Weiske J, Badock V, Tauber R, Bommert K, Huber O. Cleavage and shedding of E-cadherin after induction of apoptosis. J Biol Chem. 2001; 276:4972–80. [PubMed: 11076937]

18. Weiske J, Schoneberg T, Schroder W, Hatzfeld M, Tauber R, Huber O. The fate of desmosomal proteins in apoptotic cells. J Biol Chem. 2001; 276:41175–81. [PubMed: 11500511]

19. Elmore S. Apoptosis: a review of programmed cell death. Toxicol Pathol. 2007; 35:495–516. [PubMed: 17562483]

20. Andrade R, Crisol L, Prado R, Boyano MD, Arluzea J, Arechaga J. Plasma membrane and nuclear envelope integrity during the blebbing stage of apoptosis: a time-lapse study. Biol Cell. 2010; 102:25–35. [PubMed: 19630753]

21. Croft DR, et al. Actin-myosin-based contraction is responsible for apoptotic nuclear disintegration. J Cell Biol. 2005; 168:245–55. [PubMed: 15657395]

22. Piret JP, Lecocq C, Toffoli S, Ninane N, Raes M, Michiels C. Hypoxia and $CoCl_2$ protect HepG2 cells against serum deprivation- and t-BHP-induced apoptosis: a possible anti-apoptotic role for HIF-1. Exp Cell Res. 2004; 295:340–9. [PubMed: 15093734]

23. Zou W, et al. Cobalt chloride induces PC12 cells apoptosis through reactive oxygen species and accompanied by AP-1 activation. J Neurosci Res. 2001; 64:646–53. [PubMed: 11398189]

24. Lindahl PE, Oberg KE. The effect of rotenone on respiration and its point of attack. Exp Cell Res. 1961; 23:228–37. [PubMed: 13762256]

25. Wolvetang EJ, Johnson KL, Krauer K, Ralph SJ, Linnane AW. Mitochondrial respiratory chain inhibitors induce apoptosis. FEBS Lett. 1994; 339:40–4. [PubMed: 8313978]

26. Deng YT, Huang HC, Lin JK. Rotenone induces apoptosis in MCF-7 human breast cancer cell-mediated ROS through JNK and p38 signaling. Mol Carcinog. 2010; 49:141–51. [PubMed: 19777565]

27. Jung JY, Kim WJ. Involvement of mitochondrial- and Fas-mediated dual mechanism in $CoCl_2$-induced apoptosis of rat PC12 cells. Neurosci Lett. 2004; 371:85–90. [PubMed: 15519734]

28. Li N, et al. Mitochondrial complex I inhibitor rotenone induces apoptosis through enhancing mitochondrial reactive oxygen species production. J Biol Chem. 2003; 278:8516–25. [PubMed: 12496265]

29. Cronier L, et al. Connexin expression and gap junctional intercellular communication in human first trimester trophoblast. Mol Hum Reprod. 2002; 8:1005–13. [PubMed: 12397213]

30. Cronier L, et al. Requirement of gap junctional intercellular communication for human villous trophoblast differentiation. Biol Reprod. 2003; 69:1472–80. [PubMed: 12826585]

31. Dunk CE, et al. The molecular role of connexin 43 in human trophoblast cell fusion. Biol Reprod. 2012; 86:1–10.

32. Prise KM, Folkard M, Michael BD. A review of the bystander effect and its implications for low-dose exposure. Radiation protection dosimetry. 2003; 104:347–55. [PubMed: 14579891]

33. Andrade-Rozental AF, Rozental R, Hopperstad MG, Wu JK, Vrionis FD, Spray DC. Gap junctions: the "kiss of death" and the "kiss of life". Brain Res Rev. 2000; 32:308–15. [PubMed: 10751679]

34. Huang X, et al. Cell to cell contact required for bystander effect of the TNF-related apoptosis-inducing ligand (TRAIL) gene. Int J Oncol. 2003; 22:1241–5. [PubMed: 12738989]

35. Vines AM, Lyng FM, McClean B, Seymour C, Mothersill CE. Bystander effect induced changes in apoptosis related proteins and terminal differentiation in *in vitro* murine bladder cultures. Int J Radiat Biol. 2009; 85:48–56. [PubMed: 19205984]

36. Burton GJ, Skepper JN, Hempstock J, Cindrova T, Jones CJ, Jauniaux E. A reappraisal of the contrasting morphological appearances of villous cytotrophoblast cells during early human pregnancy; evidence for both apoptosis and primary necrosis. Placenta. 2003; 24:297–305. [PubMed: 12657502]

37. Bhola PD, Mattheyses AL, Simon SM. Spatial and temporal dynamics of mitochondrial membrane permeability waves during apoptosis. Biophys J. 2009; 97:2222–31. [PubMed: 19843454]

38. Pacher P, Hajnoczky G. Propagation of the apoptotic signal by mitochondrial waves. EMBO J. 2001; 20:4107–21. [PubMed: 11483514]

39. Rehm M, Huber HJ, Hellwig CT, Anguissola S, Dussmann H, Prehn JH. Dynamics of outer mitochondrial membrane permeabilization during apoptosis. Cell Death Differ. 2009; 16:613–23. [PubMed: 19136937]

40. Garcia-Perez C, Roy SS, Naghdi S, Lin X, Davies E, Hajnoczky G. Bid-induced mitochondrial membrane permeabilization waves propagated by local reactive oxygen species (ROS) signaling. Proc Natl Acad Sci U S A. 2012; 109:4497–502. [PubMed: 22393005]

41. O'Connor CL, Anguissola S, Huber HJ, Dussmann H, Prehn JH, Rehm M. Intracellular signaling dynamics during apoptosis execution in the presence or absence of X-linked-inhibitor-of-apoptosis-protein. Biochim Biophys Acta. 2008; 1783:1903–13. [PubMed: 18590777]

42. Brady NR, et al. Coordinated behavior of mitochondria in both space and time: a reactive oxygen species-activated wave of mitochondrial depolarization. Biophys J. 2004; 87:2022–34. [PubMed: 15345578]

43. Brady NR, Hamacher-Brady A, Westerhoff HV, Gottlieb RA. A wave of reactive oxygen species (ROS)-induced ROS release in a sea of excitable mitochondria. Antioxid Redox Signal. 2006; 8:1651–65. [PubMed: 16987019]

Appendix. Supplementary material

Supplementary material associated with this article can be found, in the online version, at **doi:**
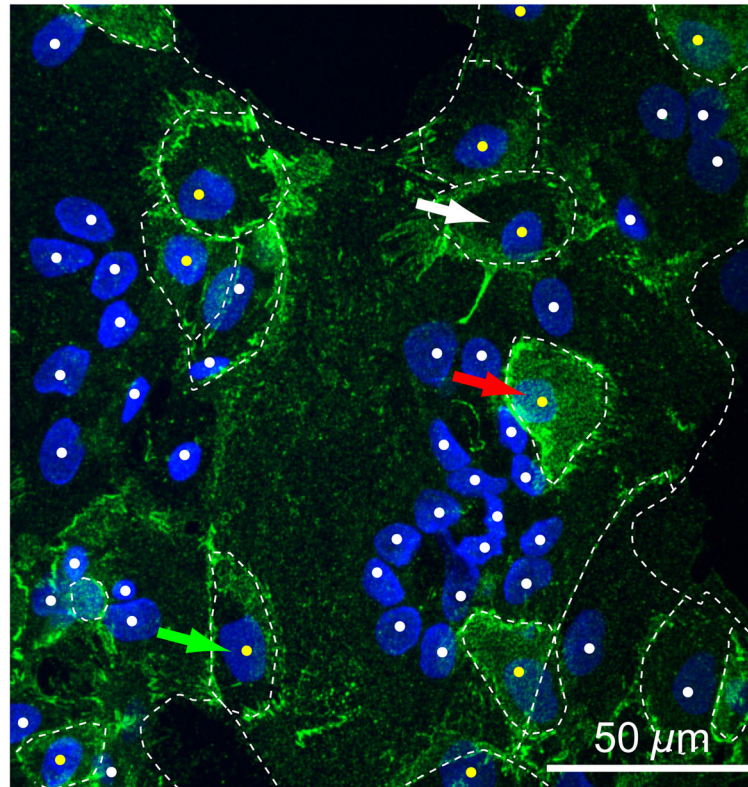
Figure 1. Structural relationships of cultured cytotrophoblasts and syncytiotrophoblast
Shown is a maximal projection of confocal Z-stacks of primary human trophoblasts cultured for 76 h in 20% O_2 and stained for E-cadherin (green) and DNA (blue). White dots indicate syncytiotrophoblast nuclei, which frequently appear clustered, and yellow dots indicate cytotrophoblast nuclei. White dotted lines indicate E-cadherin marking plasma membranes. Green arrow indicates a cytotrophoblast on the periphery of the syncytium, the red arrow indicates a cytotrophoblast that overlays the syncytium, and the white arrow indicates a cytotrophoblast within, and at the same focal plane, as the surrounding syncytium. See associated Supplementary movie 1.
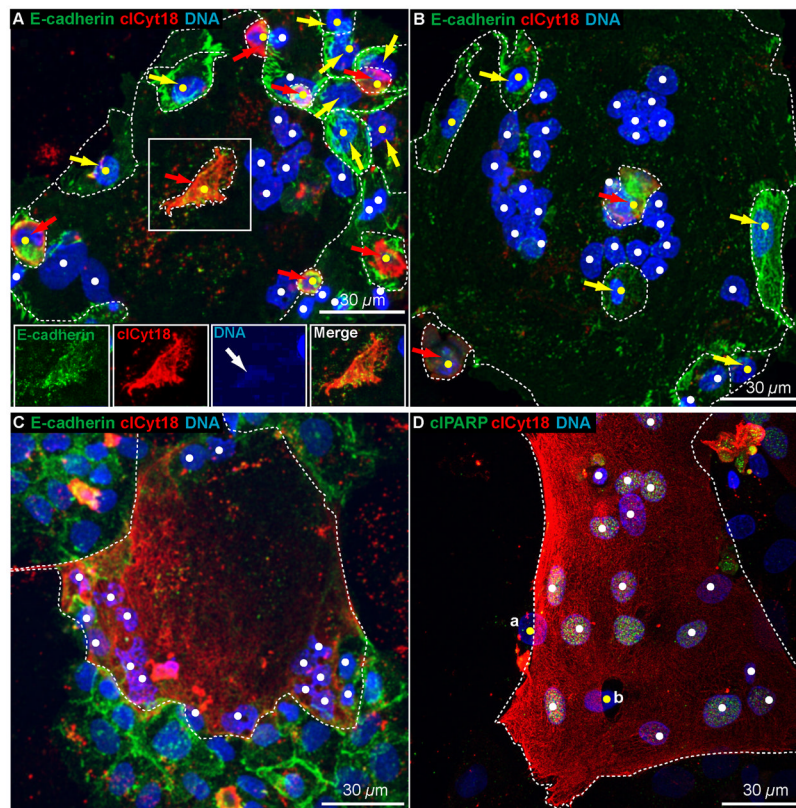
Figure 2. Apoptotic trophoblasts in fixed cells
Shown are maximal projections of confocal Z-stacks of primary human trophoblasts cultured for 76 h in 20% O_2 and stained for (A-C) E-cadherin, clCyt18 and DNA or (D) clPARP, clCyt18, and DNA, as indicated by the colored text. White dots indicate syncytiotrophoblast nuclei and yellow dots indicate cytotrophoblast nuclei. White dotted lines indicate E-cadherin marking plasma membranes. (A, B) Yellow arrows indicate non-apoptotic cytotrophoblasts and red arrows indicate apoptotic cytotrophoblasts. In (A), center boxed region is shown below as single channel and merged images to show the cytoplasmic E-cadherin demarcating the region with clCyt18, and the weakly staining, but detectable, nuclear DNA that appears fragmented and partly degraded (white arrow). In (B), the center red arrow indicates an apoptotic cytotrophoblast that overlays the syncytiotrophoblast. (A, B) see associated Supplementary movie 2. (C, D) Entire regions of syncytia were apoptotic as indicated by clCyt18 and clPARP throughout the syncytium. See associated Supplementary movie 3. In (D), the nuclei of two non-apoptotic cytotrophoblasts are visible which (a, b) partially underlay or are (b) partially surrounded by syncytiotrophoblast. See associated Supplementary movie 3.
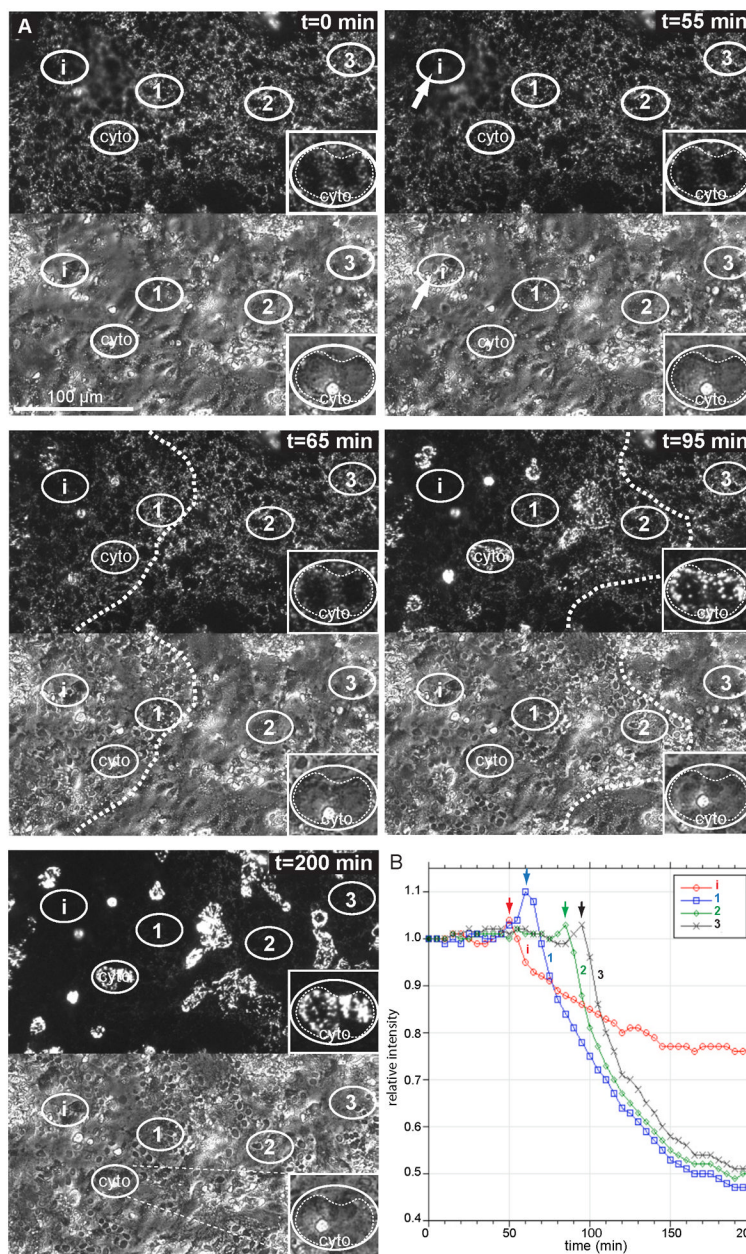
Figure 3. Live-cell imaging of progressive wave of apoptosis through syncytiotrophoblast
Shown are (A) images of selected time points by fluorescence, to follow mitochondrial depolarization by loss of JC-1 signal, and by phase contrast, to follow condensation of nuclei. In this example, apoptosis initiates in region (i), as indicated by the arrow at t = 55 min after the beginning of imaging and proceeds from left to right, eventually encompassing the entire region of the syncytium within the field of view. Mitochondrial depolarization and nuclear condensation occur simultaneously, at least within the 5 min time resolution of the imaging. i and 1–3; regions of syncytium used for quantification shown in (B). cyto, cytotrophoblast that can be identified by phase contrast imaging (inset) that shows an increase in JC-1 signal as apoptosis occurs in the adjacent syncytium. (B) Quantification over time of the JC-1 signal intensity in the region of initiation (i) and of selected regions of the syncytium (1–3, from left to right), show a transient increase in JC-1 signal (arrows) just

in front of the apoptotic wave, and then a rapid decline in JC-1 signal in the syncytium. See associated Supplementary movie 4.